www.czasopisma.pan.pl PAN www.journals.pan.pl

ARCHIVES OF ACOUSTICS
Vol. **38**, No. 4, pp. 503–516 (2013)

DOI: 10.2478/aoa-2013-0060

Numerical Evaluation of Sound Attenuation Provided by Periodic Structures

Mário MARTINS[(1)], Luís GODINHO[(2)], Luís PICADO-SANTOS[(3)]

[(1)] *I.P.C., Instituto Superior de Engenharia de Coimbra*
R. Pedro Nunes, 3030-199 Coimbra, Portugal
CIEC — Departamento de Engenharia Civil da Universidade de Coimbra
R. Luís Reis Santos, 3030-788 Coimbra, Portugal; e-mail: mariomm@isec.pt

[(2)] *CICC, Departamento de Engenharia Civil, Universidade de Coimbra*
R. Luís Reis Santos, 3030-788 Coimbra, Portugal; e-mail: lgodinho@dec.uc.pt

[(3)] *DECivil, Instituto Superior Técnico, Universidade Técnica de Lisboa*
Av. Rovisco Pais, 1049-001 Lisboa, Portugal; e-mail:picado.santos@civil.ist.utl.pt

(*received March 22, 2013; accepted October 10, 2013*)

The use of periodic structures as noise abatement devices has already been the object of considerable research seeking to understand its efficiency and see to what extent they can provide a functional solution in mitigating noise from different sources. The specific case of sonic crystals consisting of different materials has received special attention in studying the influence of different variables on its acoustic performance.

The present work seeks to contribute to a better understanding of the behavior of these structures by implementing an approach based on the numerical method of fundamental solutions (MFS) to model the acoustic behavior of two-dimensional sonic crystals. The MFS formulation proposed here is used to evaluate the performance of crystals composed of circular elements, studying the effect of varying dimensions and spacing of the crystal elements as well as their acoustic absorption in the sound attenuation provided by the global structure, in what concerns typical traffic noise sources, and establishing some broad indications for the use of those structures.

Keywords: traffic noise, sonic crystals, numerical methods.

1. Introduction

Among different types of environmental noise sources for which the national and European legislation established maximum noise exposure levels, the traffic noise, with special focus on road traffic, assumes a clear prevalence.

The World Health Organization (2011) estimates that, considering the different impacts associated with noise, the losses, expressed in Disability-Adjusted Life Year (DALY), reach a value between 1.0 and $1.6 \cdot 10^6$, i.e. at least a million years of healthy life are lost annually as a result, mostly due to traffic noise.

Another study on the situation held in the Netherlands (den Boer, Schroten, 2007) indicates that the annual loss (in 2000) due to traffic noise was approximately 40 DALY $\times 1000$ inhabitants, and this value already accounted for about half of the total result of traffic accidents. Moreover, the same study mentions the growing trend of the effects of traffic noise, whereas on traffic accidents the tendency is to decrease.

Being relatively consensual as for the need to invest in interventions that can offset the negative effects of this type of noise, generically one can distinguish between interventions at three different levels: at the generation (the vehicle-tire-pavement interaction), at the propagation medium (the area surrounding the roads), and at the reception of noise (the characteristics of the facades of buildings in the vicinity of roads).

Fitting into the second of the above types of interventions, the use of 'classical' noise barriers is usually considered an effective solution to reduce sound levels, by between 5 and 10 dB, but whose performance depends essentially on the geometry and the sound absorption characteristics of their surfaces.

This work intends to contribute to the analyses of a different approach in the use of these barriers which consists in using a periodic arrangement of vertical cylindrical elements organized in a geometric configuration such as to attenuate the incident sound levels, with particular emphasis on certain frequencies. This solution is commonly known as "sonic crystal".

Sonic crystals get their name by analogy with ordered structures of semiconductor materials such as silicon crystals whose feature of allowing certain energy waves to pass through and block others is transposed, in sonic crystals, into the capacity to prevent or limit the propagation of certain sound frequencies. The shape of these structures corresponds to a "grid" or "lattice" consisting of a base element which is repeated regularly in one, two, or three dimensions.

It is generally considered that the first evidence that it was possible to achieve some effect of acoustic obstruction using structures in periodic arrays was derived fortuitously from a sculptural element, in the gardens of the *Fundación Juan March* in Madrid, consisting of a number of vertical metal tubes arranged in a rectangular grid. A series of measurements conducted in 1995 by placing a set of microphones along this sculpture revealed clear effects in attenuating certain frequency bands of sounds which were a function of the direction of incident sound waves (Martinez-Sala *et al.*, 1995).

Since then, different aspects of the behavior of sonic crystals have been studied, some of which were essentially theoretical, while others focused on some potential practical applications. In the first group, aspects such as the influence of so called point defects (Wu *et al.*, 2009) or the existence of waveguides in which the sound propagates with low attenuation (Vasseur *et al.*, 2008) can be mentioned. In the field of the practical uses of sonic crystals, one which may be regarded perhaps as the most promising is their precise use for the selective attenuation of sound, for example as traffic noise barriers (Sánchez-Pérez *et al.*, 2002). A very recent work on this topic (Castiñeira-Ibáñez *et al.*, 2012) has addressed the classification of sonic crystal barriers in terms of relevant European standards for the determination of the intrinsic characteristics of acoustic barriers. Although a limited set of tests was performed in that work, the results have shown that the sonic crystal barriers can be acoustically competitive when compared with classic noise barriers used to mitigate traffic noise.

The underlying principle behind the latter case has to do with the aforementioned fact that these periodic structures have an attenuation capacity in certain frequency bands of sounds and with the fact that the dominant frequencies in road traffic noise can also be identified. Thus, by being designed to match those frequencies, such structures could provide a very effective way to mitigate traffic noise.

This application presents some advantages when compared to conventional noise barriers such as the fact that it does not require foundations as significant as the latter, due to its comparatively small mass, and the relatively small action of the wind, as it is a fairly "open" structure (Castiñeira-Ibáñez *et al.*, 2012). Another important benefit is the ability to adapt its attenuation capabilities to a specific site's requirements through an appropriate "fine tuning" of geometrical configuration of the elements in its periodic structure.

As a disadvantage, it should be noted that to achieve an attenuation level similar to that of a traditional noise barrier, a structure with a significant thickness may be required. A possible solution could arise by combining different effects, such as multiple scattering resonances or sound absorption capabilities in the sonic crystal (Romero García, 2010). There are, moreover, some experiments in this direction, for example the use of porous coatings on individual cylindrical of elements sonic crystals (Umnova *et al.*, 2006) or the use of trees arranged in different periodic geometrical configurations in order to achieve noise attenuation outdoor (Martínez-Sala *et al.*, 2006).

A relatively consensual aspect, from the available published literature, is that these periodic structures provide a certain level of sound attenuation due to two different mechanisms: the geometry of the structure itself and also the acoustic properties of the scatterers, for example their sound absorption. What is also apparently clear is that the study of the combined effect of these two aspects, in order to correctly predict the level of sound attenuation results, is not a trivial procedure.

Although a significant number of works has been published, the subject of sonic crystals is still under development and there are several issues that need further studying. In what concerns the numerical modeling of these structures, some benefits can be taken from adapting concepts inherited from other areas of acoustics and wave propagation, namely in what concerns the theoretical and numerical treatment of the problem. This paper is, thereby, intended as a contribution to the development of the study in this area, proposing a general numerical strategy based on the Method of Fundamental Solutions (MFS) to model a 2D sonic crystal noise barrier subjected to the incidence of acoustic waves generated by a line source. First, the theoretical formulation in which the numerical analysis methodology is based will be presented; the proposed model will then be verified against reference solutions; a set of results will be further laid out, depicting different combinations of geometrical and acoustic absorption characteristics, followed by main conclusions and some indications regarding further work.

2. Mathematical formulation

In the present work, MFS is adopted to perform numerical simulations. Essentially, MFS is a collocation technique which requires only the definition of a set of points along the physical boundaries of the problem to establish an approach to its solution. Based on these points and making use of a linear combination of fundamental solutions of the differential equation governing the problem, the method allows to obtain, in a simple manner, an approximation to the solution. As in the better-known Boundary Element Method, MFS requires previous knowledge of the fundamental solutions which are not always known to the type of the problem involved; obtaining these solutions is mathematically complex and can be extremely difficult in the case of nonlinear problems with moving boundaries or time dependence. Still, the mathematical approach of MFS is much simpler than that of the BEM, since its formulation does not require performing any kind of integrations, analytically or numerically, within the domain or along the boundary. This method has been discussed in the literature by various authors. Noteworthy are the works of Fairweather and Karageorghis (1998), Fairweather *et al.* (2003), or Golberg and Chen (1999). It should be noted that, despite its simplicity, many of the published works show that MFS can provide a very accurate calculation of solutions for different physical problems, including those related to the field of acoustics (Alves, Valtchev, 2005; Godinho *et al.*, 2007; António *et al.*, 2008) and wave propagation (Godinho *et al.*, 2009).

The following sections summarize the main aspects of the method when applied to solving acoustical problems in the frequency domain.

2.1. Governing equation

It is usual to consider that the propagation of sound in a two-dimensional space, in the frequency domain, can be represented mathematically by the Helmholtz equation. This equation has the usual form

$$\nabla^2 p + k^2 p = 0, \tag{1}$$

where $\nabla^2 = \dfrac{\partial}{\partial x^2} + \dfrac{\partial}{\partial y^2}$, p is the acoustic pressure, $k = \omega/c$, $\omega = 2\pi f$, f is the frequency, and c is the propagation velocity within the acoustic medium.

2.2. Fundamental solution

Given the differential equation (1), it becomes possible to define analytical solutions that satisfy the equation under certain conditions. One such situation corresponds to free-field conditions in which the medium is considered infinite and for which a two-dimensional pressure field is generated by a sound source located at point $\boldsymbol{x}_0$ of coordinates (x_0, y_0). This solution, known as the fundamental solution, allows to define the acoustic field in terms of pressure and particle velocities generated by the source at any receiver located at point $\boldsymbol{x}$ of coordinates (x, y) as

$$G^{2D}(\boldsymbol{x}, \boldsymbol{x}_0, k) = -\frac{i}{4}\mathrm{H}_0^{(2)}(kr), \tag{2}$$

$$H^{2D}(\boldsymbol{x}, \boldsymbol{x}_0, k, \mathbf{n}) = \frac{k}{-4\rho\omega}\mathrm{H}_1^{(2)}(kr)\frac{\partial r}{\partial \mathbf{n}}, \tag{3}$$

where $r = \sqrt{(x - x_0)^2 + (y - y_0)^2}$, and $\mathbf{n}$ represents the direction along which the particle velocity is to be calculated.

2.3. MFS formulation

In MFS, the solution of the problem is approximated by a linear combination of fundamental solutions. To formulate the method, consider a generic problem governed by Eq. (1) where the problem's physical boundary $\Gamma = \Gamma_1 \cup \Gamma_2$ (see Fig. 1) can be subjected to either Dirichlet or Neumann boundary conditions defined, respectively, by:

$$p = p_K \quad \text{at} \quad \Gamma_1, \tag{4}$$

$$-\frac{1}{i\rho\omega}\frac{\partial}{\partial \mathbf{n}}p = v_K \quad \text{at} \quad \Gamma_2. \tag{5}$$

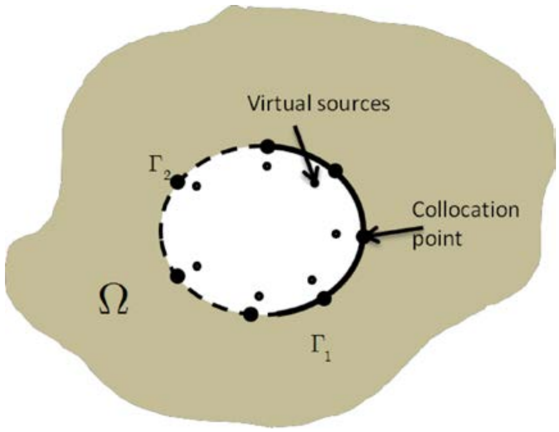

Fig. 1. Schematic representation of the problem.

In the general case, it is not a trivial task to compute a solution that simultaneously satisfies these prescribed boundary conditions together with Eq. (1). To allow obtaining one such solution, consider a set of *NS* virtual sources located outside the field of analysis, and assume that the pressure field at any domain point $\boldsymbol{x}$ can be represented by a linear combination of the effects of *NS* sources positioned at points $\boldsymbol{x}_j$, so that

$$p(\boldsymbol{x}, k) = \sum_{j=1}^{NS} Q_j G(\boldsymbol{x}, \boldsymbol{x}_j, k), \tag{6}$$

where Q_j is an amplitude factor associated with each of the virtual sources and which is, *a priori*, unknown.

For the problem under study, and given such representation of the pressure field, consider, additionally, a set of NC collocation points distributed along the boundary (see Fig. 1). Imposing the desired boundary conditions (Eqs. (4) and (5)) at each of the NC collocation points, two sets of equations can be written:

$$\sum_{j=1}^{NS} Q_j G(\boldsymbol{x}_i, \boldsymbol{x}_j, k) = p_{K,i} \quad \text{for each } \boldsymbol{x}_i \text{ at } \Gamma_1, \tag{7}$$

$$\sum_{j=1}^{NS} Q_j H(\boldsymbol{x}_i, \boldsymbol{x}_j, k, \mathbf{n}) = v_{K,i} \quad \text{for each } \boldsymbol{x}_i \text{ at } \Gamma_2, \tag{8}$$

where $p_{K,i}$ and $v_{K,i}$ are the sound pressure and the normal particle velocity values, respectively, to be prescribed at each collocation point i.

Establishing these equations, a system with NC equations for NS unknowns can be written, allowing the calculation of the unknown amplitude factors Q_j. If $NS = NC$, a linear equation system is obtained for which the solution can be calculated making use of common solution procedures such as the Gauss elimination.

It is worth noting that besides the two boundary conditions indicated in Eqs. (4) and (5), it is sometimes useful to impose mixed, or Robin, boundary conditions. In acoustics, this can be the case of absorbing boundaries to which surface impedance Z is ascribed. In that situation, the boundary condition can be written as

$$\frac{p}{i/\rho\omega \times \partial p/\partial \mathbf{n}} = Z. \tag{9}$$

To enforce this boundary condition, a combination of Eqs. (7) and (8) must be written for the relevant collocation points, which becomes

$$\sum_{j=1}^{NS} \left[Q_j G(\boldsymbol{x}_i, \boldsymbol{x}_j, k) - Z Q_j H(\boldsymbol{x}_i, \boldsymbol{x}_j, k, \mathbf{n}) \right] = 0. \tag{10}$$

3. Model verification

To verify and assess the accuracy of the proposed MFS model described in the previous section, two different configurations will be here analyzed corresponding to systems with one or multiple inclusions.

As a first test, consider that the system includes just a single circular inclusion placed within an infinite fluid medium with density of 1.22 kg/m^3 and allowing sound to propagate at 340 m/s. The circular inclusion has a rigid surface and exhibits a radius of 0.1 m, being centered at ($x = 0.0$ m; $y = 0.0$ m); this inclusion is illuminated by a source located at ($x = -0.5$ m; $y = 0.0$ m), and the response is determined at a set of receivers located over a circumference of radius 0.2 m, with the same center as the inclusion. This configuration is illustrated in Fig. 2a.

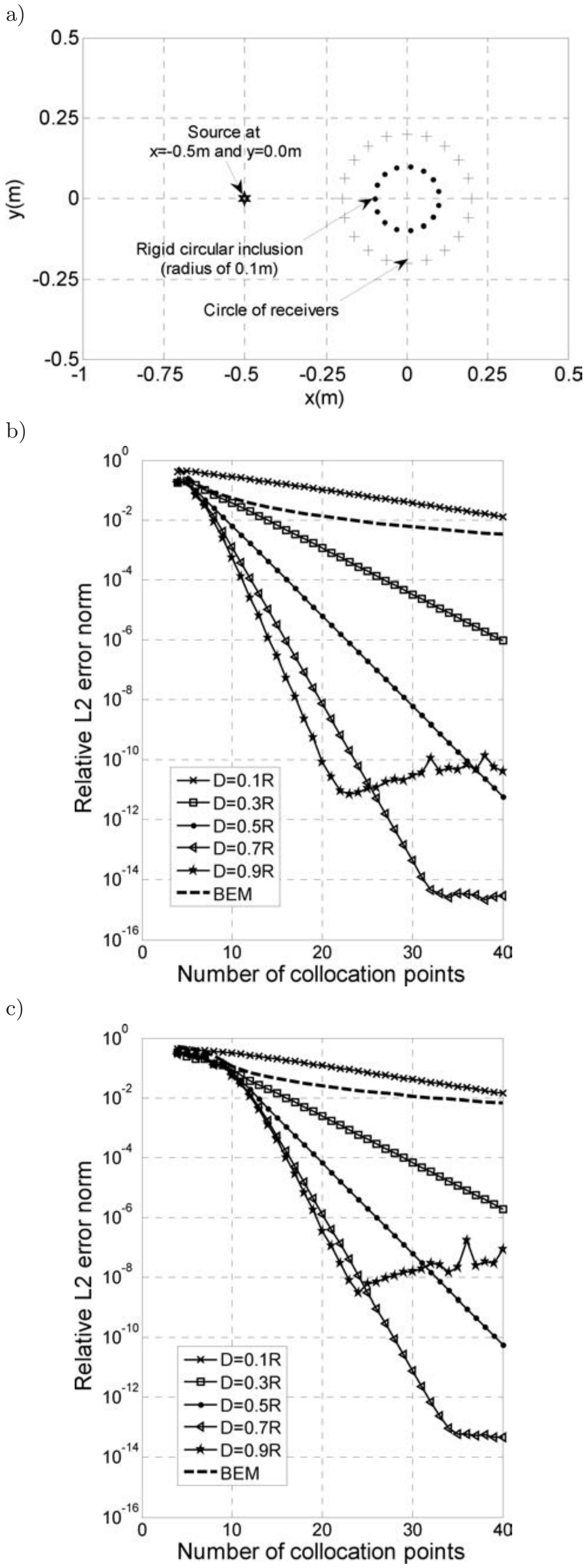

Fig. 2. Geometry of the model (a) and convergence results when analyzing a single rigid circular inclusion with a radius of 0.1 m. Results are shown for 1 kHz (b) and 2 kHz (c).

To analyze the proposed configuration, MFS is here used, positioning the virtual sources inside the inclusion, equally spaced along a circumference; different distances between these sources and the boundary are tested ranging from $0.1R$ to $0.9R$. Figures 2b and 2c illustrate the relative L2 error norm computed for frequencies of 1 kHz and 2 kHz, for different numbers of collocation points; as a reference for the calculation of this error, an analytical solution of this problem is used based on works of Tadeu *et al.* (2001). In addition, a similar curve is presented for the more classic BEM model, also for increasingly refined discretizations. It should be noted that each of these plots can be viewed as a set of convergence curves computed for each of the considered distances, and thus gives important information related to numerical behavior of the method.

Analyzing the two figures, it can be observed that MFS presents very good convergence rates for all analyzed distances, clearly surpassing the behavior of the BEM for this test case. Moreover, one can conclude that by positioning the sources at larger distances from the boundary leads to increasingly better results, reaching excellent convergence rates for distances equal or larger than $0.5R$. The best convergence rates are obtained when the sources are positioned as far from the boundary as possible (e.g. concentrated near the center); however, for this case, the convergence curve reaches a point above which the results do not improve with the increase in the number of collocation points, since the equation system becomes progressively more ill-conditioned, affecting the quality of the results.

A second test case was analyzed to verify the proposed model, corresponding to a more complex configuration in which eight circular inclusions, each of them with a radius of 0.1 m, are illuminated by a source located at the same position as indicated above; in addition, Robin boundary conditions (as defined in Eq. (9)) with $Z = 1000$ Pa·s/m are imposed along all boundaries. For this case, results are computed using MFS with 15 collocation points (and positioning the virtual sources at a distance $0.5R$) and BEM with 30 boundary elements. The response is computed at a line of receivers located at $x = 1.0$ m. Figure 3a illustrates the proposed configuration.

Figure 3b exhibits the calculated results for a frequency of 2 kHz, over the indicated line of receivers. Here, a perfect match between the two numerical methods can be seen, revealing the excellent behavior of MFS in the analysis of this specific type of problem, even when Robin conditions are considered. It should also be noted that the finer discretization required by BEM, together with the need to perform integrations over each boundary element, leads to a much higher computational effort of this method when compared with MFS.

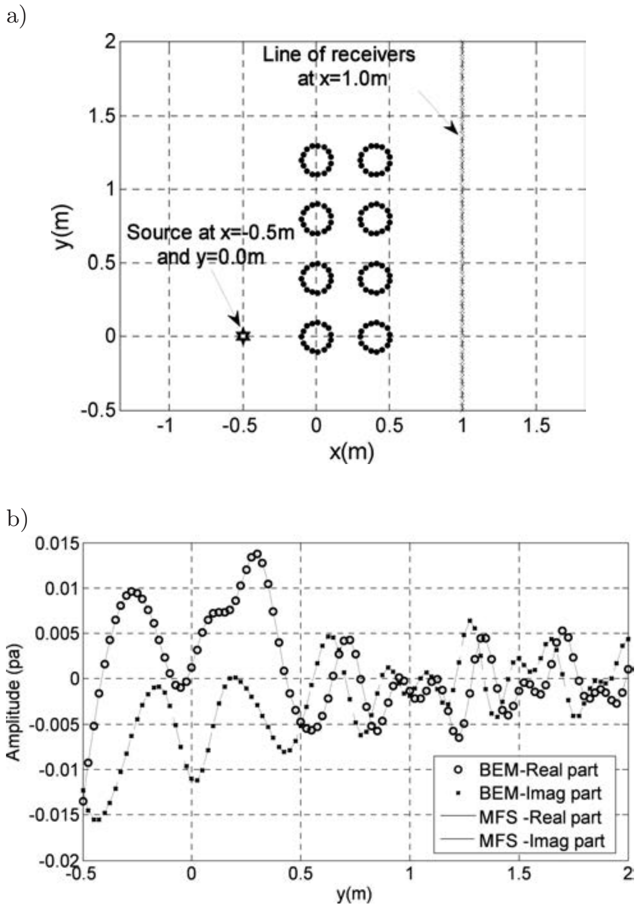

Fig. 3. Comparison with the results computed using a BEM model for 2 kHz when the geometry consists of eight circular inclusions (a) with Robin boundary conditions. The results (b) are computed using 30 boundary elements (BEM) or 15 collocation points (MFS) to discretize each circle.

4. Discussion of numerical results

As previously mentioned, the main mechanisms by which sonic crystals provide specific levels of sound attenuation or insertion loss, are the geometry of its basic periodic structure, or lattice, and the acoustic properties of its individual scatterer elements. In what follows, the proposed MFS formulation is applied to analyze the influence of different combinations of those aspects when a periodic structure is used as a noise barrier alongside a road, as illustrated in Fig. 4.

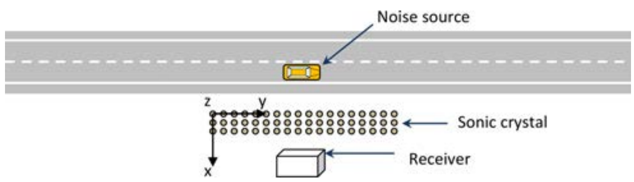

Fig. 4. General configuration for the studied cases.

For this purpose, the traffic assumes the role of the noise source, a small area (a window for example) of a nearby house shall correspond to the receiver, and a sonic crystal noise barrier will be located between them, materialized by a set of vertical cylinders, either rigid or with some level of acoustic absorption. Those cylinders are considered to be arranged in two distinct lattice configurations, typical of sonic crystals, namely square or triangular, as shown in Fig. 5.

a)

b)

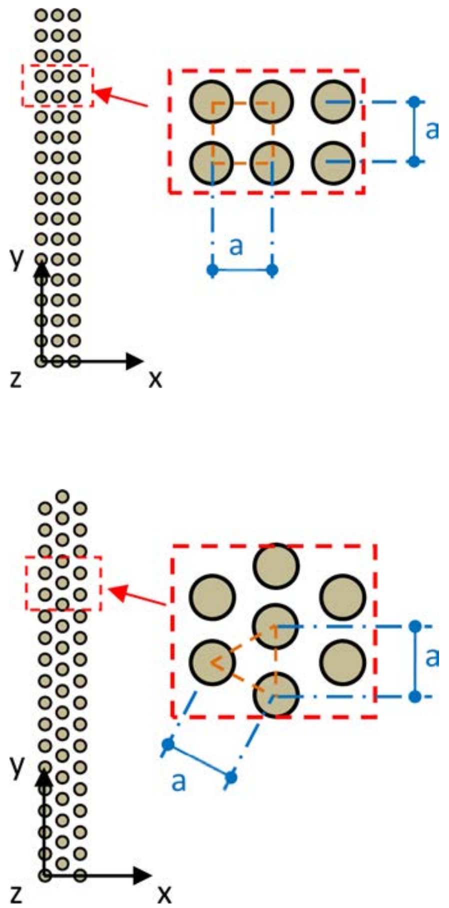

Fig. 5. Square (a) and triangular (b) lattice configurations of the sonic crystal.

Throughout the different analyses presented in the following, the situation shown above is studied by means of frequency domain responses calculated on a horizontal plane, as the geometry of the problem can be considered constant along the z-axis (vertical). For such a case, the MFS model described in the previous sections can be used to simulate the pressure field around the structure of the sonic crystal.

In order to replicate a realistic situation, based on the usual dimensions from a typical cross section of a road, the positions of the source and receivers will correspond, in the axis system shown in Fig. 4, respectively, to values of $x = -6.5$ m and $x = 7.5$ m. As for the y-axis values, the analyses were made considering the receiver close to the center of the barrier along that axis (consisting of five distinct receiver points along a length of 0.80 m). The source was initially assumed to be located in front of the receiver (at half the length of the crystal), although in further calculations its location will additionally be considered in other positions.

The analysis carried out sought to evaluate the influence in the sonic crystal's sound attenuation features for different geometrical parameters (the number of cylinders in the sonic crystal, the diameter of the cylinders, the spacing between cylinders, the position of the noise source and also the random variability of the diameter of the cylinders) as well as the acoustic absorption characteristics of the scatterers.

4.1. Influence of the number of cylinders

As the intention is to examine the attenuation related to road traffic noise, given that it is usual to consider that this noise exhibits a maximum sound level near 1000 Hz (Sandberg, 2003), at this stage the attenuation values evaluated corresponded to five individual frequencies in the region of this maximum, specifically 600, 800, 1000, 1200, and 1400 Hz.

In analyzing the influence of the number of cylinders, the purpose is to establish the minimum number of scatterers that can provide nearly stable levels of attenuation at those frequencies, for each of the two lattice configurations previously mentioned. Along the y-axis, that number will correspond to the smallest "length" along that direction so that the diffraction effect near the extremities of the structure becomes negligible. In trying to keep the solutions as economical as possible, the "width" of the sonic crystals, along the x-axis, will be kept at two or three cylinders.

Consequently, N being the number of cylinders along the y-axis, we will have arrangements for each of the cases of $2N$ cylinders or $3N$ cylinders.

As for the other geometrical parameters of the sonic crystals, given that they are supposed to embody road noise barriers, to avoid very dense structures and ensure the cylindrical elements are sufficiently robust but have a plausible dimension if obtained from trees, the diameter of the cylinders was assumed to be 0.20 m, and the distance between the centers of cylinders, i.e. the lattice constant, $a = 0.40$ m.

The sound attenuation was then evaluated for each of the five frequencies already mentioned, for increases in the number of cylinders along the y-axis, in multiples of five, until the values of the sound attenuation can be perceived stabilizing for the various frequencies, indicating that negligible diffraction phenomena occur at edges of the sonic crystals. The results are summarized in Figs. 6 and 7.

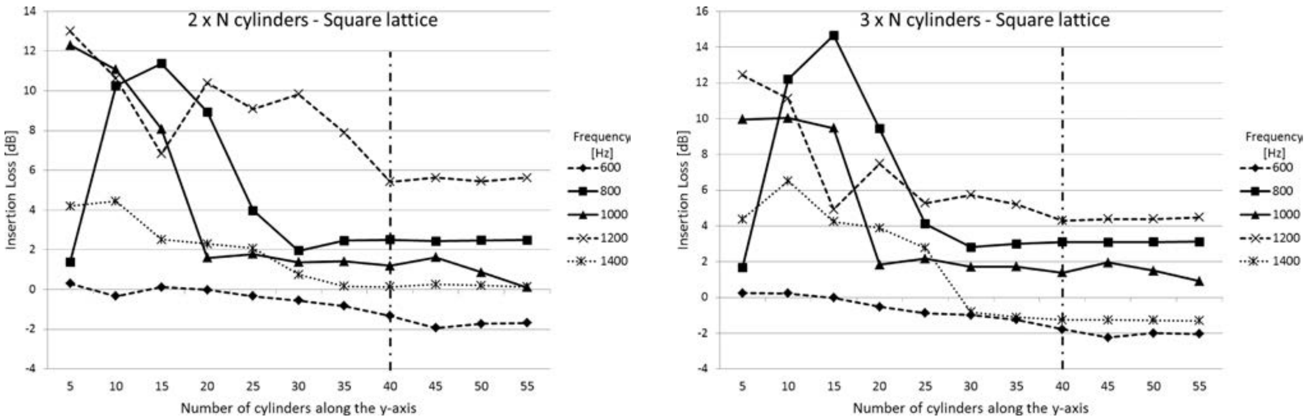

Fig. 6. Insertion Loss (in dB) vs number of cylinders (square configuration).

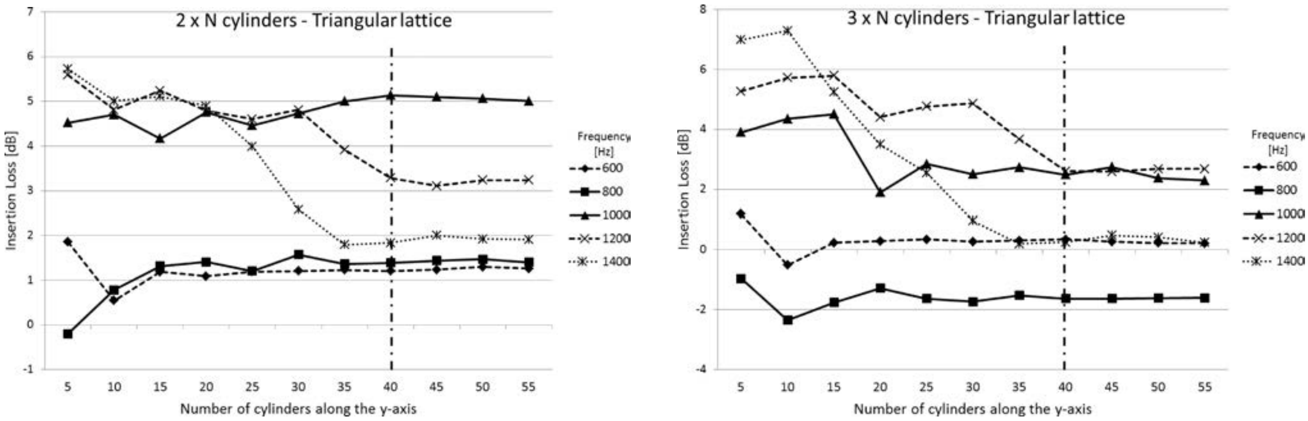

Fig. 7. Insertion Loss (in dB) vs number of cylinders (triangular configuration).

In view of these results, the minimum numbers of cylinders along the y-axis for the different configurations under consideration were established as follows:

- Square configuration:

  $2N = 40$ cylinders / $3N = 40$ cylinders;
- Triangular configuration:

  $2N = 40$ cylinders / $3N = 40$ cylinders.

From this point on, the attenuation values are obtained by means of an energetic average within each of five 1/3 octave frequency bands with centers at 630, 800, 1000, 1250, and 1600 Hz. For this purpose, frequencies between 562.5 Hz and 1777.5 Hz, with an increment of 7.5 Hz, were analyzed.

4.2. Influence of the diameter of the cylinders

In this case, assuming sonic crystals with the number of cylinders established in the preceding section for different lattice configurations and maintaining $a = 0.40$ m, the attenuation values were calculated considering diameters of 0.20, 0.15, and 0.10 m. The results are shown in Figs. 8 and 9, referring to the center frequency of the five 1/3 octave frequency bands defined above.

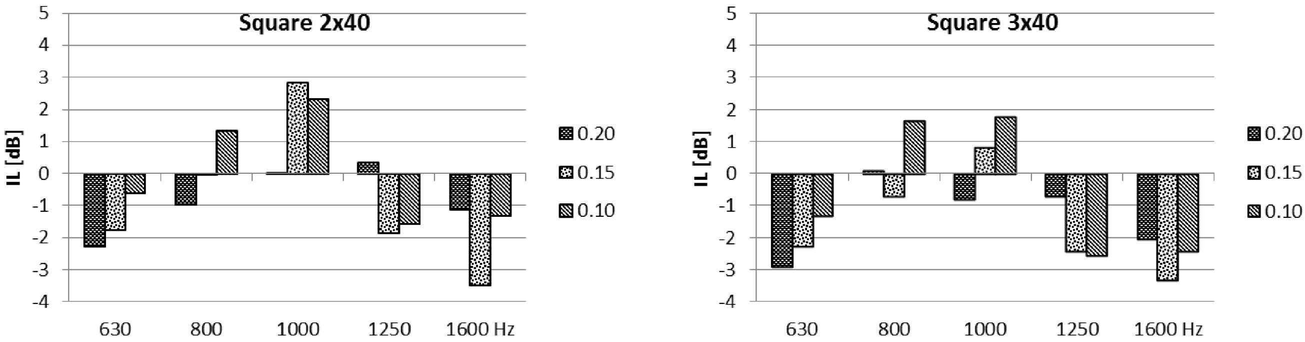

Fig. 8. Insertion Loss (in dB) vs diameter of cylinders (square configuration).

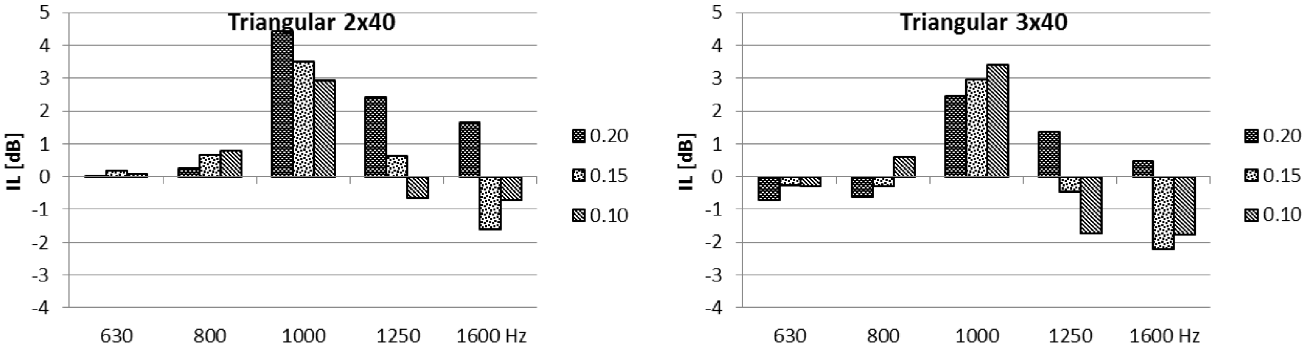

Fig. 9. Insertion Loss (in dB) vs diameter of cylinders (triangular configuration).

From these values, a noticeably higher attenuation can be seen to occur when the triangular lattice configurations (particularly the one with 2×40 cylinders) are used. Indeed, for those configurations, peak attenuation values at the frequency band of 1000 Hz are observable, with insertion loss values as high as 4.5 dB. Interestingly, and mostly for the square lattice configuration, negative values of the *IL* (amplification) may be observable which can be strongly related to the fact that the source and the receivers are at similar positions in the y-axis. For that case, the sound may travel directly through the gap between cylinders which could have a waveguide-type effect generating some amplification.

4.3. Influence of the spacing between the cylinders

Assuming, once again, sonic crystals with the dimensions used in the preceding point and cylinders with a diameter of 0.20 m, the influence of the distance between the centers of cylinders, i.e. the lattice constant a, was analyzed. The sound attenuation corresponding to values for that spacing of 0.50, 0.40, and 0.30 m, for the different configurations, was determined, and the results are shown in Figs. 10 and 11.

The main conclusion that can be drawn from these figures is that variation of the lattice constant induces

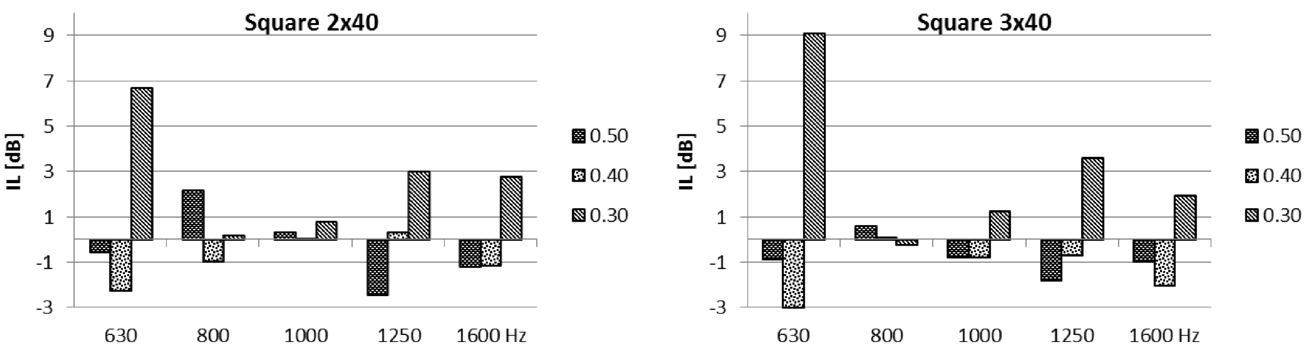

Fig. 10. Insertion Loss (in dB) vs lattice constant a (square configuration).

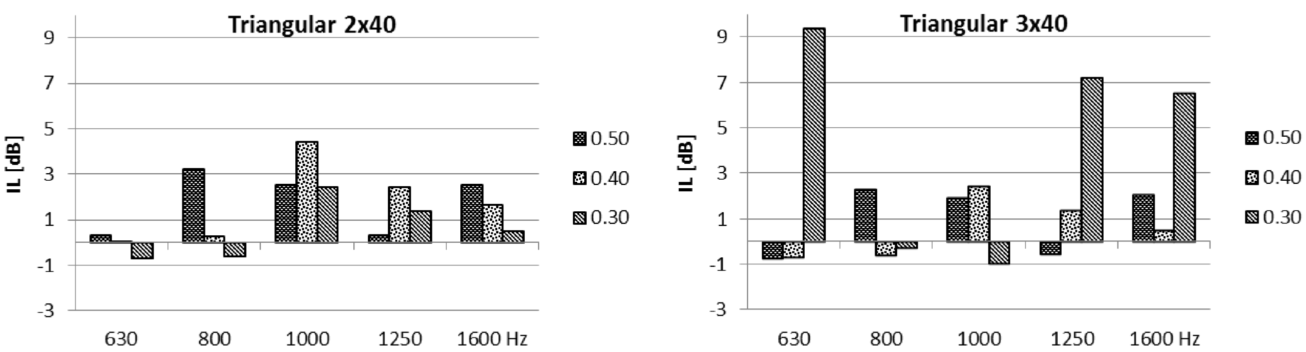

Fig. 11. Insertion Loss (in dB) vs lattice constant a (triangular configuration).

very pronounced variations of performance in terms of attenuation. There is no clear advantage of any of the tested scenarios, which makes it difficult to identify the best choice. However, it can be stated that, in these results, the smaller attenuation provided by the square configuration compared to the triangular one is again very clear.

Comparing the results computed for the three values of the lattice constant it can be seen that strong variations occur between the tested cases. Indeed, although the smaller value (0.3 m) seems to provide better results when the square lattice is used, in some cases it seems to be outperformed by other values of this spacing. As an example, observing the results for the triangular lattice with 3×40 elements, it is possible to conclude that this spacing is clearly inadequate when analyzing the 800 Hz and 1000 Hz frequency bands; by contrast, on the lower and higher frequency bands, the results reveal a very good efficiency, with high values of the *IL*.

4.4. Influence of the random variability of the cylinders' diameter

The possibility of using natural resources, such as timber logs, to build a sonic crystal noise barrier could mean using scatterers that are not entirely identical concerning their diameter.

Therefore, in the present section the aim is to investigate if small diameter variations can produce a substantial difference in terms of the sound attenuation provided by the structure. In the presented results, a lattice constant of 0.40 m is assumed.

For each of the lattice configurations under study, a possible maximum random variation of 10 and 20% of the reference diameter (0.20 m) is analyzed. The computed sound attenuation values are presented in Figs. 12 and 13. In the cases where random variations of the diameters are assumed, the results correspond to an average of three separate computations. One should note that the random variation in those cases is applied separately for each element of the structure, thus generating structures with heterogeneous elements. From the presented results, only small differences of sound attenuation seem to occur when random variations of the diameter of the scatterer elements exist. Indeed, even when a maximum 20% diameter variation is assumed, the calculated insertion loss values are only very slightly changed, with maximum variations of less than 0.5 dB in all analyzed frequency bands.

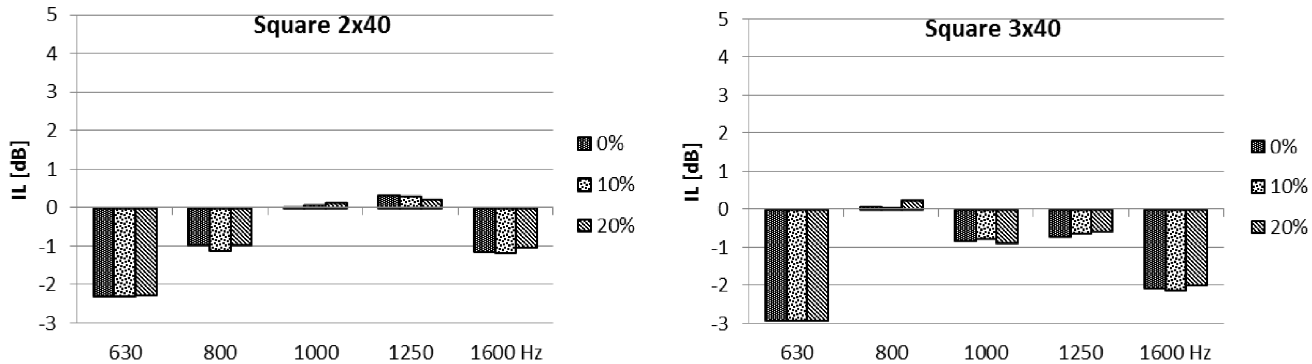

Fig. 12. Insertion Loss (in dB) vs diameter variability (square configuration).

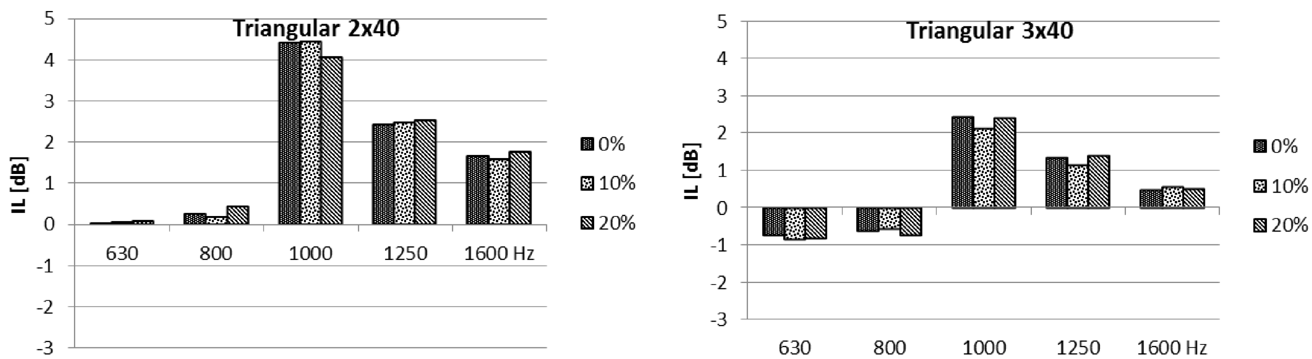

Fig. 13. Insertion Loss (in dB) vs diameter variability (triangular configuration).

4.5. Influence of the incidence angle of the sound waves

As stated above, the relative position of source and receivers can generate significant changes in the sound attenuation results. This topic is addressed in the present section by trying to find out how a longer path and different obstructions from the scatterers affect the sound attenuation at the receiver. The noise source was considered in three different positions, related to the "length" L of the sonic crystal, namely $y = 0$, $y = 1/4L$, and $y = 1/2L$ (which was the position assumed in the preceding sections), as shown in Fig. 14.

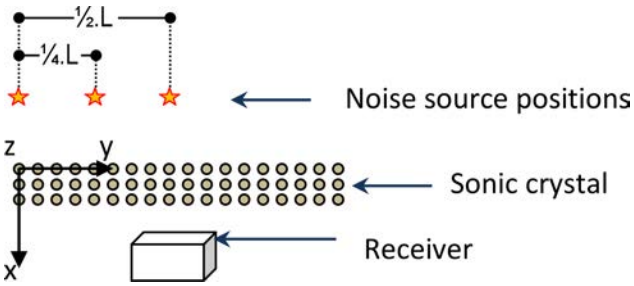

Fig. 14. Different positions of the noise source.

For each of the three positions of the source, the sound attenuation values for the five frequency bands were calculated. The resulting calculations, related to the different lattice configurations, with $a = 0.40$ m and cylinders with 0.20 m in diameter, are presented in Figs. 15 and 16.

The presented results clearly reveal the strong influence of the relative position of source and receivers. As the source is positioned nearer to the extremity of the sonic crystal (further away from the receiver), the insertion loss computed for the square lattice becomes progressively higher. As stated before, when the source and receivers are aligned around the same y-coordinates, a direct travel path may exist and almost no attenuation is observed. This path no longer seems to exist when the source is positioned further from the receivers' position, and thus higher attenuation values are generated. In the presence of triangular lattices, a similar, but less evident, effect is also seen. For that case, the most prominent feature is that the attenuation reaches higher values for the lower frequency bands, for which insertion loss values of more than 8 dB (for the 3×40 triangular configuration) may be observed.

4.6. Influence of the acoustic absorption of the cylinders

Taking into consideration the possible use of cylinders made of different materials, the effect of different sound absorption coefficients (α) was also studied. Attenuation values were computed for each of the three

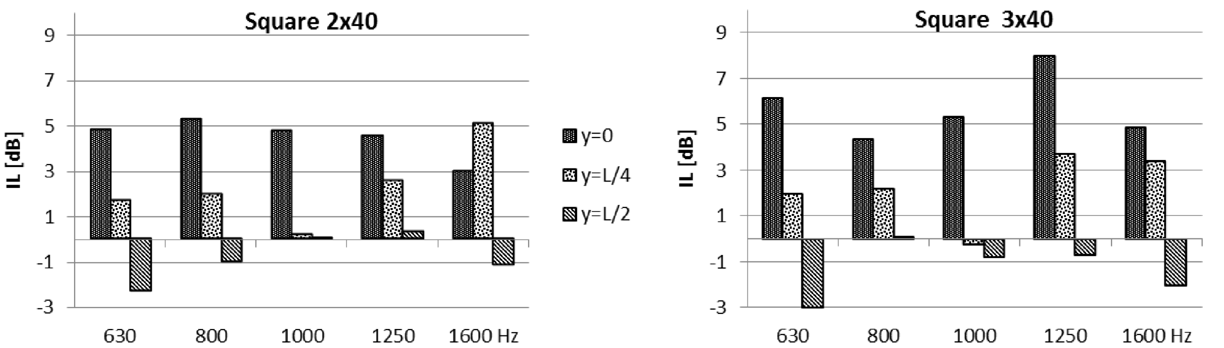

Fig. 15. Insertion Loss (in dB) vs noise source position (square configuration).

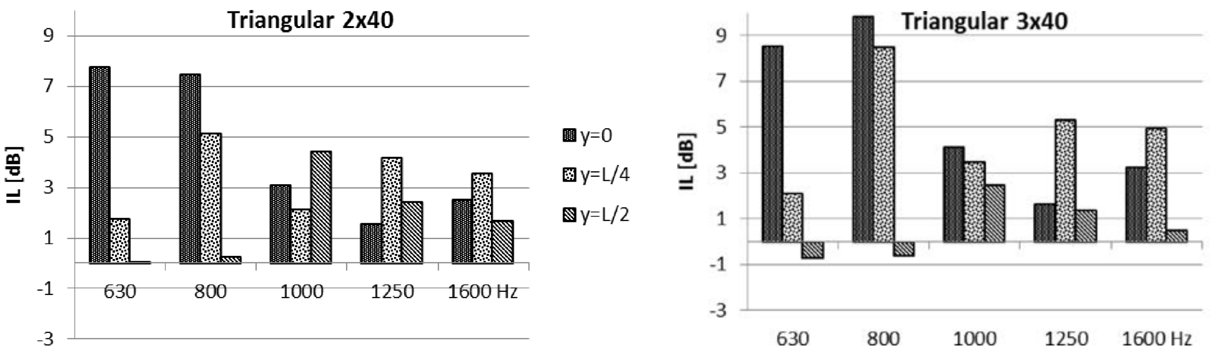

Fig. 16. Insertion Loss (in dB) vs noise source position (triangular configuration).

positions of the noise source discussed in the previous section. The results are presented in Figs. 17 and 18, for $\alpha = 0.1$, 0.3, and 0.5. To implement these values of the absorption coefficient, Robin boundary conditions are considered at boundaries of each cylinder. A real-valued impedance given by

$$Z = \rho\, c \frac{1+\sqrt{1-\alpha}}{1-\sqrt{1-\alpha}}, \tag{11}$$

with $c = 340$ m/s and $\rho = 1.22$ kg/m^3, is then considered.

In Fig. 17, corresponding to results computed for the square lattice, it can be observed that by progressively increasing the sound absorption coefficient, increased values of the insertion loss are obtained throughout the studied frequency bands. This fact was very much expected, since the presence of an absorbing surface allows sound energy to be progressively dissipated whenever one of those surfaces is hit by acoustic waves. Curiously, the effect of those absorbing surfaces is also quite significant when the source and the receivers are aligned, which indicates that the waveguide effect referred before is strongly attenuated by those absorbent materials. Indeed, observing the results for the higher absorption coefficient ($\alpha = 0.5$) it can be seen that interesting values of the insertion loss are computed for all source positions, representing a marked improvement when compared with the results computed for $\alpha = 0.1$. For this case ($\alpha = 0.5$), peak insertion loss values are reached at 1000 Hz (for the 2×40 structure) and 1250 Hz (for the 3×40 structure), for which *IL* values of 10 dB and 15 dB are reached when the source is further away from the receivers, and of 4 dB and 6 dB when the source is aligned with those receivers. These attenuation values can be seen as noteworthy in what concerns traffic noise attenuation.

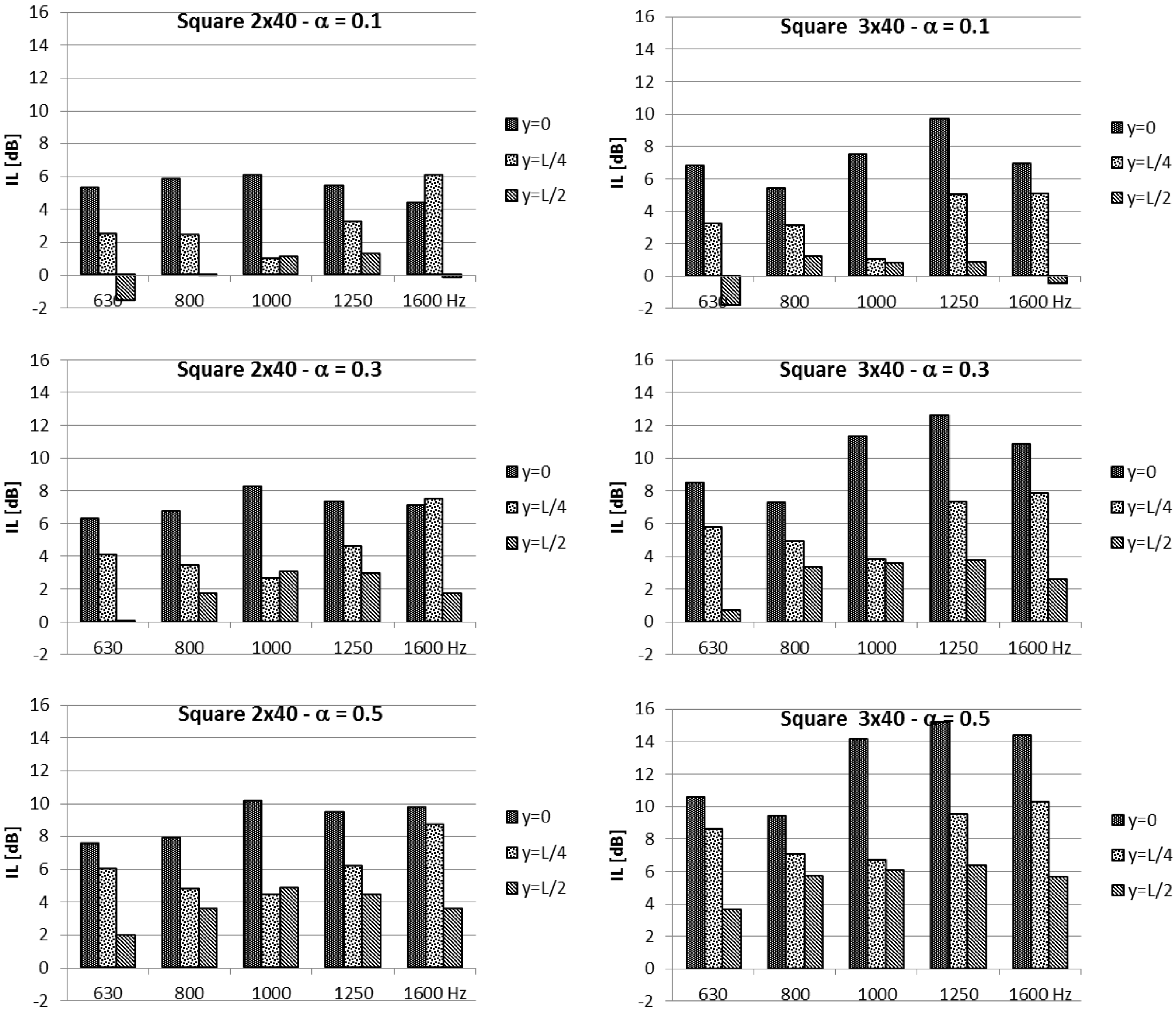

Fig. 17. Insertion Loss (in dB) vs noise source position (square configuration) for varying values of the absorption coefficient.

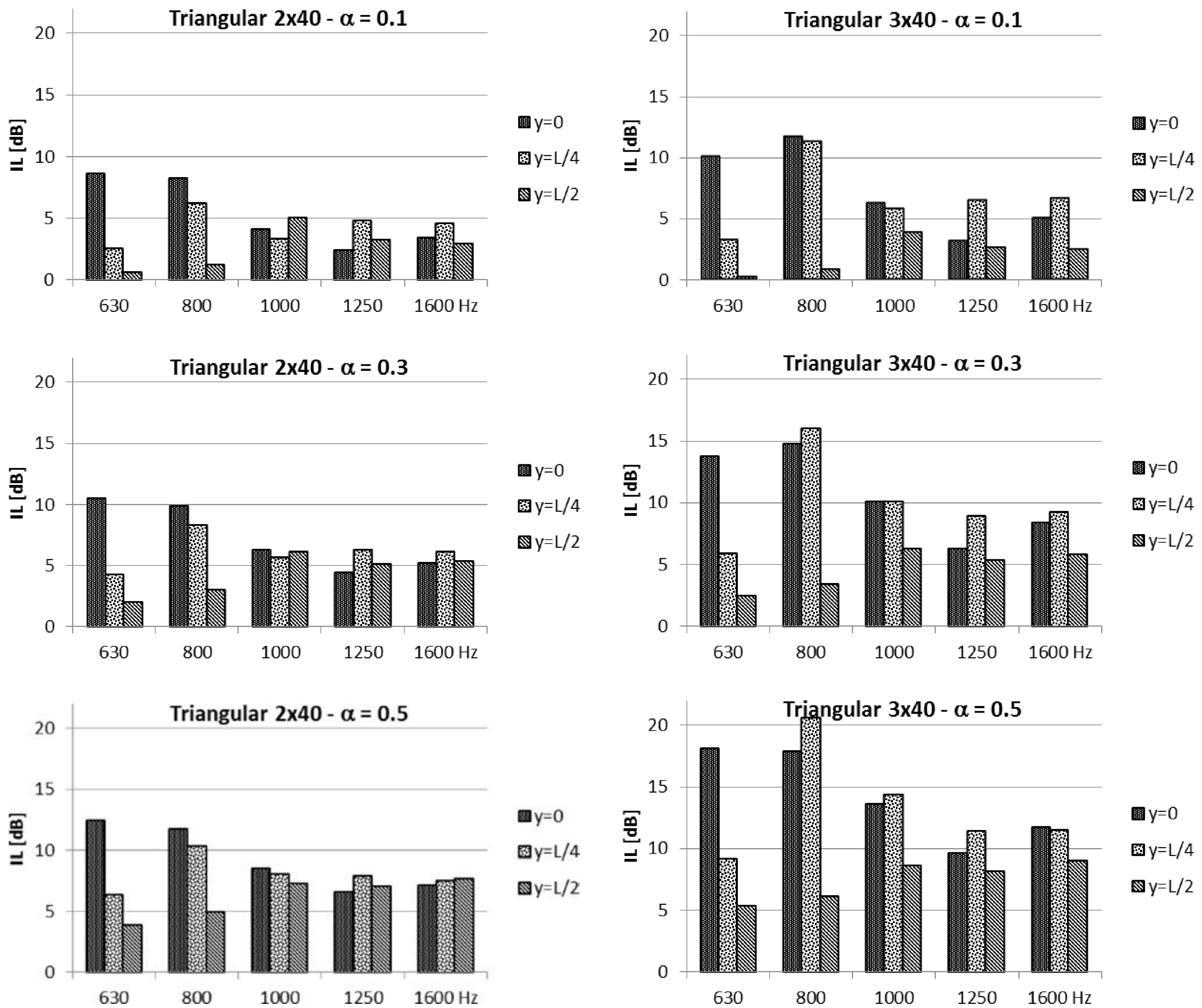

Fig. 18. Insertion Loss (in dB) vs noise source position (triangular configuration) for varying values of the absorption coefficient.

Finally, the results in Fig. 18 illustrate the evolution of the attenuation for the case of the triangular lattice. For this case, the conclusions that may be drawn are, globally, very similar to those stated for the square lattice. However, as the computed values of the insertion loss are, generally, higher for this configuration, this seems to suggest that in an actual road barrier application, the triangular configuration might be considered more adequate.

5. Final remarks

The present work addressed the use of sonic crystals as noise barriers to mitigate road traffic noise by means of an approach based on a numerical technique called the Method of Fundamental Solutions. This technique was adopted, as it appeared to be particularly well suited to the requirements of the topic being studied, largely due to the geometric characteristics of the structures employed.

The accuracy of the model in evaluating the sound pressure in the presence of multiple cylindrical inclusions is analyzed by benchmarking the results against those computed using the better known Boundary Element Method. The comparison yielded very favorable indications in favor of MFS, namely regarding discretization of the problem and computation times, compared with those when BEM was used.

Several arrangements were studied, covering different combinations of geometrical and acoustic absorption characteristics, and the influence of those aspects in the resulting attenuation values provided by the sonic crystals was analyzed, allowing some broad indications to be established. For example, when comparing the effect of using a triangular or square lattice, the results seem to show a trend for better performance, in terms of the calculated insertion loss, when structures with a triangular lattice configuration are used.

Another apparently clear implication of the results is the influence of the location of the noise source on the overall sound attenuation. When assuming the source's position in different locations, noticeable variations of the insertion loss are registered at the receiver's position, which appears to suggest the possible existence of some sort of waveguide action. As this can lead to highly divergent outcomes, from the receiver's point of view, such possibility should be thoroughly examined by carrying out additional analyses.

The results presented in this work appear to indicate that the use of MFS may have a good potential to be employed in further research in this subject. Future developments will predictably include the analysis of more complex arrangements, regarding both the geometrical parameters of the periodic structure and acoustical properties of the scatterers. Another relevant topic for further development is related with the three-dimensional effect of the sonic crystal which, in a real configuration, has a limited height and thus may also be affected by diffraction effects occurring at its top. From a more experimental point of view, further investigation will certainly be required in terms of laboratory and field tests, using physical models, to allow the validation of the numerical results.

Acknowledgments

The research work presented herein was supported by FEDER funds through the Operational Programme for Competitiveness Factors – COMPETE and by national funds through the FCT (Portuguese Foundation for Science and Technology), under research project PTDC/ECM-COM/1438/2012.

This paper represents a development with increased detail of a paper presented at the VIII Iberomerican Acoustics Congress, VII Iberian Acoustics Congress, XLIII Spanish Acoustics National Congress – TECNIACÚSTICA® 2012 and Acoustics European Symposium, organized by the Sociedade Portuguesa de Acústica (SPA) and the Sociedad Española de Acústica (SEA), with the support of the European Acoustics Association (EAA), the Federação Iberoamericana de Acústica (FIA), the International Commission for Acoustics (ICA), the Laboratório Nacional de Engenharia Civil (LNEC), and the University of Évora.

References

1. Alves C.J.S., Valtchev S.S. (2005), *Numerical comparison of two meshfree methods for acoustic wave scattering*, Engineering Analysis with Boundary Elements, **29**, 4, 371–382.

2. António J., Tadeu A., Godinho L. (2008), *A three-dimensional acoustics model using the method of fundamental solutions*, Engineering Analysis with Boundary Elements, **32**, 525–531.

3. den Boer L.C., Schroten A. (2007), *Traffic noise reduction in Europe – Health effects, social costs and technical and policy options to reduce road and rail traffic noise*, Delft.

4. Castiñeira-Ibáñez S., Rubio C., Romero-García V., Sánchez-Pérez J.V., García-Raffi L.M. (2012), *Design, Manufacture and Characterization of an Acoustic Barrier Made of Multi-Phenomena Cylindrical Scatterers Arranged in a Fractal-Based Geometry*, Archives of Acoustics, **37**, 4, 455–462.

5. Fairweather G., Karageorghis A. (1998), *The method of fundamental solutions for elliptic boundary value problems*, Adv. Comput. Math., **9**, 69–95.

6. Fairweather G., Karageorghis A., Martin P. (2003), *The method of fundamental solutions for scattering and radiation problems*, Engineering Analysis with Boundary Elements, **27**, 759–769.

7. Godinho L., Amado Mendes P., Tadeu A., Cadena-Isaza A., Smerzini C., Sánchez Sesma F., Madec R., Komatitsch D. (2009), *Numerical Simulation of Ground Rotations along 2D Topographical Profiles under the Incidence of Elastic Plane Waves*, Bulletin of the Seismological Society of America, **99**, 2B, 1147–1161.

8. Godinho L., Tadeu A., Amado Mendes P. (2007), *Wave propagation around thin structures using the MFS*, Computers Materials, Continua (CMC), **5**, 2, 117–127.

9. Golberg M., Chen C.S. (1999), *The method of fundamental solutions for potential, Helmholtz and diffusion problems. Boundary Integral Methods: Numerical and Mathematical Aspects*, Computational Engineering, vol. 1. Boston, MA: WIT Press/Computational Mechanics Publications, pp. 103–176.

10. Martinez-Sala R., Rubio C., Garcia-Raffi L.M., Sanchez-Perez J.V., Sanchez-Perez E.A., Llinares J. (2006), *Control of noise by trees arranged like sonic crystals*, Jour. Sound Vib., **291**, 100.

11. Martínez-Sala R., Sancho J., Sánchez J.V., Gómez V., Llinares J., Meseguer F. (1995), *Sound attenuation by sculpture*, Nature, 378, 241.

12. Romero García D. (2010), *On the control of propagating acoustic waves in sonic crystals: analytical, numerical and optimization techniques*, Doctoral Thesis.

13. Sánchez-Pérez J.V., Rubio C., Martínez-Sala R., Sánchez-Grandia R., Gómez V. (2002), *Acoustic barriers based on periodic arrays of scatterers*, Appl. Phys. Lett., **81**, 5240.

14. Sandberg U. (2003), *The Multi-Coincidence Peak around 1000 Hz in Tyre/Road Noise Spectra*, Euronoise, Naples.

15. Tadeu A., Godinho L., António J. (2001), *Benchmark Solution for 3D Scattering from Cylindrical Inclusions*, Journal of Computational Acoustics, **9**, 4, 1311–1328.

16. Umnova O., Attenborough K., Linton C.M. (2006), *Effects of porous covering on sound attenuation by periodic arrays of cylinders*, J. Acoust. Soc. Am., **119**, 1.

17. Vasseur J.O., Deymier P.A, Djafari-Rouhani B., Pennec Y., Hladky-Hennion A-C. (2008), *Absolute forbidden bands and waveguiding in two-dimensional phononic crystal plates*, Phys. Rev. B, **77**, 085415.

18. World Health Organizatiom – Regional Office for Europe (2011), *Burden of disease from environmental noise*, Frank Theakston [Ed.], ISBN: 978 92 890 0229 5.

19. Wu L.-Y., Chen L.-W., Liu C.-M. (2009), *Acoustic pressure in cavity of variously sized two-dimensional sonic crystal with various filling fraction*, Phys. Lett. A, **373**, 1189–1195.